

Constraining the QCD phase diagram by tricritical lines at imaginary chemical potential

Philippe de Forcrand^{1,2*} and Owe Philipsen^{3†}

¹*Institut für Theoretische Physik, ETH Zürich, CH-8093 Zürich, Switzerland*

²*CERN, Physics Department, TH Unit, CH-1211 Geneva 23, Switzerland*

³*Institut für Theoretische Physik, Johann-Wolfgang-Goethe-Universität, 60438 Frankfurt am Main, Germany*

(Dated: October 30, 2018)

We present unambiguous evidence from lattice simulations of QCD with three degenerate quark species for two tricritical points in the (T, m) phase diagram at fixed imaginary $\mu/T = i\pi/3 \bmod 2\pi/3$, one in the light and one in the heavy mass regime. These represent the boundaries of the chiral and deconfinement critical lines continued to imaginary chemical potential, respectively. It is demonstrated that the shape of the deconfinement critical line for real chemical potentials is dictated by tricritical scaling and implies the weakening of the deconfinement transition with real chemical potential. The generalization to non-degenerate and light quark masses is discussed.

PACS numbers: 05.70.Fh, 11.15.Ha, 12.38.Gc

Keywords: QCD phase diagram

The QCD phase diagram is at present largely unknown. It describes which different forms of nuclear matter exist for different choices of temperature and baryon density, and whether they are separated by phase transitions. Its knowledge is thus of great importance for current and future experimental programs in nuclear and heavy ion physics as well as astro-particle physics. Since QCD is strongly coupled on scales of a baryon mass and below, fully non-perturbative calculations are warranted. Unfortunately, Monte Carlo simulations of lattice QCD at non-vanishing baryon density are prohibited by the “sign” problem. To date only indirect methods are available, introducing additional approximations which are justified for $\mu/T \lesssim 1$ only [1]. One of these consists of simulating QCD at imaginary chemical potential $\mu = i\mu_i$ with $\mu_i \in \mathbb{R}$, for which there is no sign problem, and analytically continuing the results to real chemical potential [2, 3]. While the Monte Carlo results contain the full information about imaginary μ , analytic continuation via truncated polynomials fitted to the data introduces the approximation.

In this letter we propose instead to study the phase diagram of QCD at imaginary chemical potential in its own right. We shall demonstrate that there are intricate first order, triple, critical and tricritical structures, whose details depend on the number of dynamical quark flavours N_f and their respective masses m_f . These structures are *bona fide* properties of QCD and for this reason alone merit a detailed investigation. Moreover, we show that tricritical lines found at imaginary chemical potential, with their associated scaling behaviour, represent important constraints for the critical surfaces at real chemical potential. Finally, the phase diagram we investigate may serve as benchmark for studies within effective models (such as PNJL, sigma models, quark hadron models etc.), which can be easily extended to imaginary μ .

Here we present a study of the (T, m) phase structure of QCD at fixed imaginary chemical potential $(\mu/T)_c =$

$i(2n+1)\pi T/3, n = 0, \pm 1, \pm 2, \dots$ for $N_f = 3$ degenerate quark flavours. At those values of μ , QCD undergoes a transition between adjacent $Z(3)$ sectors. This is due to the exact symmetries of the partition function,

$$Z(\mu) = Z(-\mu), \quad Z\left(\frac{\mu}{T}\right) = Z\left(\frac{\mu}{T} + i\frac{2\pi n}{3}\right), \quad (1)$$

for complex μ [4]. The different $Z(3)$ -sectors can be distinguished by the Polyakov loop

$$L(\mathbf{x}) = \frac{1}{3} \text{Tr} \prod_{\tau=1}^{N_\tau} U_0(\mathbf{x}, \tau) = |L| e^{-i\varphi}, \quad (2)$$

whose phase φ cycles through $\langle \varphi \rangle = n(2\pi/3), n = 0, 1, 2, \dots$ as the different sectors are traversed.

Hence, for imaginary $\mu = i\mu_i$ there is a global $Z(3)$ symmetry, even in the presence of finite mass quarks. Its spontaneous breaking implies transitions between neighbouring sectors for the mentioned critical values. These are first order phase transitions for high temperatures and analytic crossovers for low temperatures [2–4], as shown schematically in Fig. 1 (left). For $\mu = i\pi T$ the order parameter to distinguish between the phases is the imaginary part of the Polyakov loop, $\text{Im}(L)$. At high temperature there is a two-phase coexistence with fluctuations about $\langle \text{Im}(L) \rangle = \pm\sqrt{3}/2$, on either side of the boundary. At low temperatures $\text{Im}(L)$ fluctuates smoothly between those values. The situation is identical for the other critical values of μ_i , up to $Z(3)$ rotations.

Away from a critical value of μ_i , there is a chiral/deconfinement transition line separating high and low temperature regions. This line represents the analytic continuation of the chiral/deconfinement transition at real μ . Its nature depends on the number of quark flavours and masses. Early evidence [2, 3] is consistent with this line meeting the $Z(3)$ transition at its endpoint between first order and crossover, and our present analy-

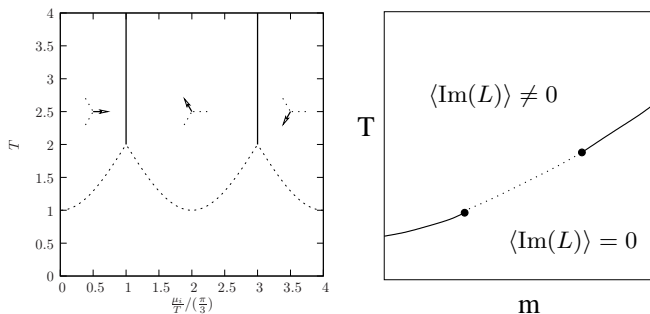


FIG. 1: Left: phase diagram for imaginary μ . Vertical lines are first order transitions between different $Z(3)$ -sectors, arrows indicate the phase of the Polyakov loop. The $\mu = 0$ chiral/deconfinement transition continues to imaginary chemical potential, its order depends on N_f and the quark masses. Right: phase diagram for $N_f = 3$ at fixed $\mu = i\pi T$. Solid lines are lines of triple points ending in tricritical points, which are connected by a $Z(2)$ -line.

sis unambiguously confirms this. The nature of the endpoint of the $Z(3)$ transition line has already been investigated for $N_f = 4$ [6] and more recently for $N_f = 2$ [5].

In this letter we study the nature of this junction at fixed $\mu = i\pi T$ in $N_f = 3$ QCD as a function of quark mass. There are three possibilities, which we shall find to be all realised. For small masses the chiral transition is first order and branches off the $Z(3)$ -transition line, rendering the meeting point of the three first order lines a triple point. For intermediate masses, the $Z(3)$ transition ends in a second order endpoint with 3d Ising universality, i.e. the chiral/deconfinement transition in its vicinity is a crossover. For large masses there is a first order deconfinement transition meeting the $Z(3)$ transition again in a triple point. Hence, for fixed $\mu = i\pi T$, we obtain a (T, m) phase diagram as in Fig. 1 (right). The endpoints of the solid lines, which separate triple points from Ising points, correspond to tricritical points.

To establish the phase diagram Fig. 1 (right) numerically, we work on lattices with temporal extent $N_t = 4$ with standard staggered fermions at fixed $\mu/T = i\pi$, using the RHMC algorithm and setting aside possible issues with taking a fractional power of the fermion determinant. For fixed N_t , temperature is tuned by varying the lattice gauge coupling β . Hence, for a given bare quark mass am , we investigate the nature of the transition as a function of β . To determine this, we analyse the finite size scaling of the Binder cumulant

$$B_4(X) \equiv \langle (X - \langle X \rangle)^4 \rangle / \langle (X - \langle X \rangle)^2 \rangle^2, \quad (3)$$

with $X = \text{Im}(L)$ and $\langle X \rangle = 0$. For $\mu/T = i\pi$, every β -value represents a point on the phase boundary and thus is pseudo-critical. In the thermodynamic limit, $B_4(\beta) = 3, 1.5, 1.604, 2$ for crossover, first order triple point, 3d Ising and tricritical transitions, respectively.

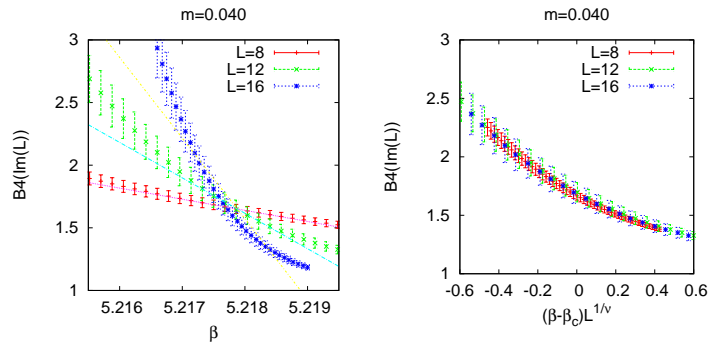


FIG. 2: Finite size scaling of B_4 for a small quark mass. On the right, the critical exponent was fixed to $\nu = 1/3$, corresponding to a first order transition.

On finite L^3 volumes the steps between these values are smeared out to continuous functions whose gradients increase with volume. The critical coupling β_c for the endpoint is obtained as the intersection of curves from different volumes. In the scaling region around a critical β_c , B_4 is a function of $x = (\beta - \beta_c)L^{1/\nu}$ alone and can be expanded as

$$B_4(\beta, L) = B_4(\beta_c, \infty) + ax + bx^2 + \dots, \quad (4)$$

up to corrections to scaling, with the critical exponent ν characterising the approach to the thermodynamic limit. The relevant values for us are $\nu = 1/3, 0.63, 1/2$ when β_c corresponds to a first order, 3d Ising or tricritical transition, respectively.

For each quark mass, we simulated lattices of sizes $L = 8, 10, 12$ (20 in a few cases), at typically 8-14 different β -values, calculated $B_4(\text{Im}(L))$ and filled in additional points by Ferrenberg-Swendsen reweighting [7]. Fig. 2 shows an example for a light quark mass $am = 0.04$. B_4 moves from large values (crossover) at low β -values (i.e. low T) towards 1 (first order transition) at large β -values (i.e. high T). In the neighbourhood of the intersection point, we then fit all curves simultaneously to Eq. (4), thus extracting $\beta_c, B_4(\beta_c, \infty), \nu, a, b$. We observe that the value of the Binder cumulant at the intersection can be far from the expected universal values in the thermodynamic limit. This is a common situation: large finite-size corrections are observed in simpler spin models even when the transition is strongly first-order [8]. Moreover, in our case, logarithmic scaling corrections will occur near a tricritical point since $d = 3$ is the upper critical dimension in this case [9]. Fortunately, the critical exponent ν , which determines the approach to the thermodynamic limit, is less sensitive to finite-size corrections and in Fig. 2 consistent with $\nu = 1/3$, its value at a first order transition. A check is to fix ν to one of the universal values and see whether the curves collapse under the appropriate rescaling, Fig. 2 (right). Note that the critical coupling determined from the intersection of the B_4 curves Fig. 2 (left) is consistent with that extracted from

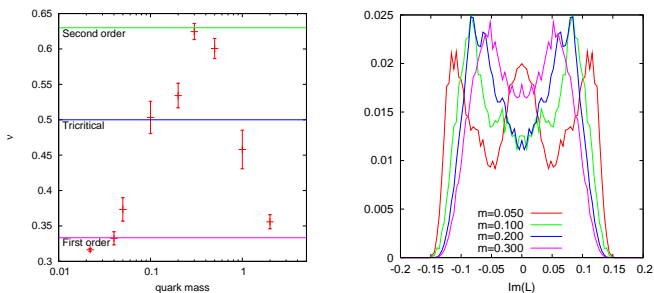


FIG. 3: Left: Critical exponent ν at $\mu/T = i\pi$. Right: Distribution of $\text{Im}(L)$ at the endpoint of the $Z(3)$ transition.

the peak of the specific heat or the chiral susceptibility.

Proceeding in this way, we have investigated quark masses distributed over a large range, with results summarised in Fig. 3 (left). We find unambiguous evidence for a change from first order scaling to 3d Ising scaling, and back to first order scaling as the quark mass is made larger. Note that, in the infinite volume limit, the curve would be replaced by a non-analytic step function, whereas the smoothed-out rise and fall in Fig. 3 (left) corresponds to finite volume corrections.

The results from the finite size scaling of B_4 can be further sharpened by looking at the probability distribution of $\text{Im}(L)$ at the critical couplings β_c , corresponding to the crossing points. This is shown in Fig. 3 (right) for masses $am = 0.05, 0.1, 0.2, 0.3$ for $L = 16$. The lightest mass displays a clear three-peak structure, indicating coexistence of three states at the coupling β_c , which therefore corresponds to a triple point. The same observation holds for heavy masses. For $am = 0.1, 0.2$ the central peak is disappearing and for $am = 0.3$ we are left with the two peaks characteristic for the magnetic direction of 3d Ising universality.

Hence, for small and large masses, we have unambiguous evidence that the boundary point between a first order $Z(3)$ transition and a crossover at $\mu = i\pi T$ corresponds to a triple point. This implies that two additional first order lines branch off the $Z(3)$ -transition line as in Fig. 1 (left), which are to be identified as the chiral (for light quarks) or deconfinement (for heavy quarks) transition at imaginary chemical potential. This is expected on theoretical grounds: for $m = 0$ or $+\infty$, these transitions are first-order for any chemical potential. The fact that the endpoint of the $Z(3)$ transition line changes its nature from a triple point at low and high masses to second order for intermediate masses implies the existence of two tricritical points. Our current data on $N_t = 4$ put these between $0.07 < am_{\text{tric1}} < 0.3$ and $0.5 < am_{\text{tric2}} < 1.5$.

Since our $N_t = 4$ lattice is very coarse, $a \sim 0.3$ fm, an important question concerns cut-off effects. These strongly affect quark masses, and thus in particular the values of the tricritical quark masses where the changes from a triple point to a critical Ising point happen. How-

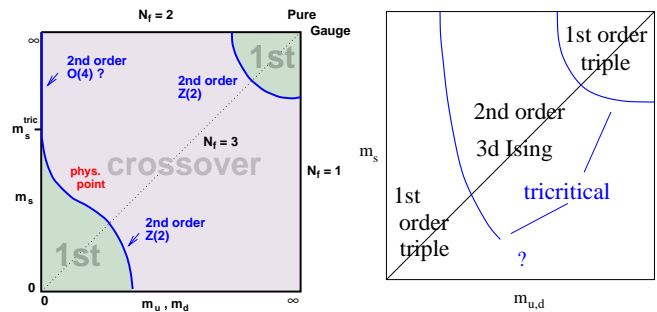


FIG. 4: Order of the transition as a function of quark masses. Left: quark hadron transition at $\mu = 0$. Right: the $Z(3)$ -transition endpoint at $\mu/T = i\pi/3$.

ever, universality implies that critical behaviour is insensitive to the cut-off, as long as the global symmetries of the theory are not changed. Our calculation is therefore sufficient to establish the qualitative picture Fig. 1 (right) for the continuum phase diagram at $\mu = i(2n + 1)\pi T/3$ for three degenerate flavours.

Let us now discuss how this critical structure is embedded in the parameter space with non-degenerate quark masses, Fig. 4 (right). The case $N_f = 3$ corresponds to the diagonal, with two tricritical points separating triple points from second order points. With non-degenerate quark masses these tricritical points will trace out tricritical lines, $m_s^{\text{tric}}(m_{u,d})$. In the case of heavy quarks the situation is qualitatively the same for any $N_f = 1, 2, 3$ [10, 11]. In the light quark regime, there is an interplay between the $Z(3)$ and chiral symmetries and the situation may be more complicated. The findings reported in [5] imply the existence of a finite tricritical light quark mass also for $N_f = 2$. It would then seem natural that the tricritical points for $N_f = 2, 3$ are continuously connected by varying the strange quark mass, though this needs to be confirmed by explicit calculations. We stress that all critical structure indicated in Fig. 4 (right) can be determined reliably with standard Monte Carlo techniques, and continuum extrapolations are feasible with current resources. Knowledge of this phase diagram in the continuum should provide valuable benchmarks for the description of the QCD phase diagram by effective models.

In order to establish the connection between imaginary and real chemical potential, let us briefly recall the situation at $\mu = 0$, Fig. 4 (left). The deconfinement transition in pure gauge theory is first order. In the presence of dynamical quarks, it weakens with decreasing quark mass until it disappears along the deconfinement critical line with 3d Ising universality. The critical point for $N_f = 1$ was determined in [11], and more recently for $N_f = 1, 2, 3$ in a strong coupling expansion for a coarse $N_t = 1$ lattice [10]. Similarly, the chiral transition for $N_f = 2 + 1$ is first order and weakens with increasing quark mass, until it disappears at a chiral critical line with 3d Ising uni-

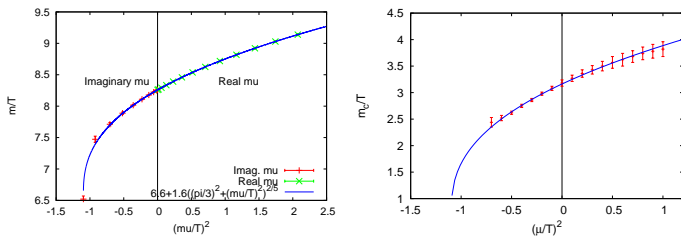


FIG. 5: Critical line $m_c(\mu^2)$ in the 3-state Potts model [14] (left) and for QCD in a strong coupling expansion [10] (right).

versality [12, 13]. When a chemical potential is switched on, these critical lines sweep out critical surfaces which continue in the imaginary μ (or $-\mu^2$) direction and join the tricritical lines at $\mu = i\pi T/3$. We shall now illustrate this for the deconfinement critical surface.

By universality, the properties of a second order transition are the same in a model sharing the same global symmetry, and for the deconfinement transition this is the 3d three-state Potts model with Hamiltonian

$$H = -k \sum_{i,\mathbf{x}} \delta_{\phi(\mathbf{x}),\phi(\mathbf{x}+\hat{i})} - \sum_{\mathbf{x}} [h\phi(\mathbf{x}) + h'\phi^*(\mathbf{x})], \quad (5)$$

where $\phi(\mathbf{x})$ is a $Z(3)$ -spin, and the couplings are identified as $h = \exp(-(M-\mu)/T)$, $h' = \exp(-(M+\mu)/T)$, while k increases with temperature. The qualitative change of the critical deconfinement line with chemical potential can be calculated in this model and one finds the first order region to shrink with real μ [14]. The same observation is made for full QCD on a coarse lattice with a strong coupling expansion [10]. See Fig. 5.

Both calculations show the continuation of the critical mass to negative μ^2 and a non-analyticity when joining the $Z(3)$ -transition at $\mu = i\pi T/3$. However, in both cases it has not been fully realised that this junction is tricritical. Since chemical potential enters the partition function of the Potts model in the same way as in QCD, it features the same $Z(3)$ -transitions. We can therefore directly check our QCD results in the heavy mass region against those in the Potts model at the same value $\mu = i\pi T/3$. For the latter, the Binder cumulant of the spin magnetisation was measured [14]. We reanalysed those data fitting them to the scaling form, Eq. (4), and indeed find a change from first order behaviour, $\nu = 0.33$, at large values of M/T to second order 3d Ising, $\nu = 0.63$, implying again a tricritical point.

Quite generally, a tricritical point represents the confluence of two ordinary critical points, i.e. in the heavy mass region the critical endpoints of the deconfinement transition at $\mu = i\pi T/3(1 \pm \varepsilon)$ merging into the $Z(3)$ endpoint at $\mu = i\pi T/3$. The deviation from the symmetry plane, $((\mu/T)^2 + (\pi/3)^2)$, corresponds to an external field in a spin model, and the way a critical line leaves a tricritical point in an external field is again governed by

universality [9],

$$\frac{m_c}{T}(\mu^2) = \frac{m_c}{T}(0) + K \left[\left(\frac{\pi}{3}\right)^2 + \left(\frac{\mu}{T}\right)^2 \right]^{2/5}. \quad (6)$$

Fig. 5 shows that the data from [14] and [10] can both be fitted to this form. An excellent description of the data is achieved, reaching far into the real chemical potential region. Thus we conclude that for heavy quark masses, the form of the critical surface of the deconfinement transition is determined by tricritical scaling of the $Z(3)$ transition at imaginary $\mu = i\pi T/3$.

It is clear that the chiral critical surface will likewise terminate on the chiral tricritical line at $\mu = i\pi T/3$. Unfortunately, for the chiral critical surface no suitable effective model for finite density is available and we presently do not know whether tricritical scaling also shapes the chiral critical surface. This could be answered conclusively by extensive simulations at intermediate values of μ_i . However, we do find $m_c(\mu = i\pi T/3) > m_c(0)$, which indicates a monotonous reduction of the critical quark mass as μ^2 is increased. This independently confirms the weakening of the first order chiral transition with real chemical potential observed previously in [2, 13, 15].

* Electronic address: forcrand@phys.ethz.ch

† Electronic address: philipsen@th.physik.uni-frankfurt.de

- [1] O. Philipsen, PoS **LAT2005** (2006) 016 [PoS **JHW2005** (2006) 012] [arXiv:hep-lat/0510077].
- [2] P. de Forcrand and O. Philipsen, Nucl. Phys. B **642**, 290 (2002) [arXiv:hep-lat/0205016].
- [3] M. D'Elia and M. P. Lombardo, Phys. Rev. D **67**, 014505 (2003) [arXiv:hep-lat/0209146].
- [4] A. Roberge and N. Weiss, Nucl. Phys. B **275**, 734 (1986).
- [5] M. D'Elia and F. Sanfilippo, arXiv:0909.0254 [hep-lat].
- [6] M. D'Elia, F. Di Renzo and M. P. Lombardo, Phys. Rev. D **76**, 114509 (2007) [arXiv:0705.3814 [hep-lat]].
- [7] A. M. Ferrenberg and R. H. Swendsen, Phys. Rev. Lett. **63**, 1195 (1989).
- [8] A. Billoire, T. Neuhaus and B. Berg, Nucl. Phys. B **396**, 779 (1993) [arXiv:hep-lat/9211014].
- [9] I.D. Lawrie and S. Sarbach, in *Phase transitions and critical phenomena*, eds. C. Domb and J.L. Lebowitz, vol.9, 1 (1984).
- [10] J. Langelage and O. Philipsen, arXiv:0911.2577 [hep-lat].
- [11] C. Alexandrou et al., Phys. Rev. D **60** (1999) 034504 [arXiv:hep-lat/9811028].
- [12] F. Karsch, E. Laermann and C. Schmidt, Phys. Lett. B **520**, 41 (2001) [arXiv:hep-lat/0107020].
- [13] P. de Forcrand and O. Philipsen, JHEP **0701**, 077 (2007) [arXiv:hep-lat/0607017].
- [14] S. Kim, Ph. de Forcrand, S. Kratochvila and T. Takaishi, PoS **LAT2005**, 166 (2006) [arXiv:hep-lat/0510069].
- [15] P. de Forcrand and O. Philipsen, JHEP **0811** (2008) 012 [arXiv:0808.1096 [hep-lat]].